Thermal Analysis and X-Ray Diffraction of Rice Husk Ash Blended Cement Under Sodium Sulfate with Wetting and Drying Cycles

P. J. Ramadhansyah, M. R. Hainin, O. Rokiah, R. Noram Irwan, W. I. Mohd Haziman, and S. A. Mangi

Abstract Sulfate attack is one of the most aggressive environmental deterioration affecting the durability of concrete structures. Thus, this study is to evaluate the effect of sodium sulfate (5% Na_2SO_4) solution on the performance of rice husk ash (RHA) blended cement under drying and wetting cycle, which is thought to simulate an aggressive environment in concrete. The RHA replacement level used was 10%. The performance of the specimen was evaluated by the differential thermal analysis (DTA), thermogravimetric analysis (TGA), and X-ray diffraction (XRD). The results showed that the replacement of ordinary Portland cement by 10% rice husk ash effectively improved the resistance of concrete due to sulfate attack. The result also indicate that the quantity of expansive gypsum formed by the reaction of calcium hydroxide will be less in RHA blended cement than in OPC specimen. In addition, RHA blended cement possibly reduced the potential of ettringite and gypsum formation due to the reduction in the quantity of calcium hydroxide, thus, improved the resistance of concrete to sulfate attack.

Keywords Sodium sulfate · RHA · XRD · Thermal · Wetting · Drying

P. J. Ramadhansyah (✉) · M. R. Hainin
Department of Civil Engineering, College of Engineering, Universiti Malaysia Pahang, 26300 Gambang, Pahang, Malaysia
e-mail: ramadhansyah@ump.edu.my

O. Rokiah · R. N. Irwan
Faculty of Civil Engineering Technology, Universiti Malaysia Pahang, 26300 Gambang, Pahang, Malaysia

W. I. M. Haziman
Faculty of Civil Engineering and Built Environment, Universiti Tun Hussein Onn Malaysia, Batu Pahat, 86400 Johor Bahru, Malaysia

S. A. Mangi
Department of Civil Engineering, Mehran University of Engineering and Technology, SZAB Campus Khairpur Mir's, Jamshoro 76060, Sindh, Pakistan

S. S. Mohd Zuki et al. (eds.), *Proceedings of the Sustainable Concrete Materials and Structures in Construction 2020*, Lecture Notes in Civil Engineering 157,
https://doi.org/10.1007/978-981-16-2187-1_15

1 Introduction

Sulfate attack is one of the most important problems concerning the durability of concrete structures [7]. The effect of sodium sulfate attack on concrete can be divided into two principal reactions: the reaction of sodium sulfate (Na_2SO_4) and the reaction of magnesium sulfate ($MgSO_4$) with calcium hydroxide [$Ca(OH)_2$] to form gypsum [14]. The formed gypsum reacts with calcium aluminate hydrates to form ettringite [15]. These reactions result in a substantial increase in volume with subsequent cracking and peeling. Based on Santhanam et al. [15], the reactions can be represented as follows:

$$Ca(OH)_2 + Na_2SO_4.10H_2O \rightarrow CaSO_4.2H_2O + 2NaOH + 8H_2O \quad (1)$$

$$2[3CaO \cdot Al_2O_3 \cdot 12H_2O] + 3[Na_2SO_4 \cdot 10H_2O] \rightarrow 3CaO \cdot Al_2O_3 \cdot 3CaSO_4 \cdot 31H_2O. + 2Al(OH)_3 + 6NaOH + 17H_2O \quad (2)$$

The reaction products are gypsum ($CaSO_4.2H_2O$) which leads to surface softening and loss of strength, and calcium sulphoaluminate ($3CaO.Al_2O_3.3CaSO_4.31H_2O$) known as ettringite which leads to considerable increase in volume [14]. According to Al-Akhras [2], the chemical interaction of sulfate attack is a complicated process and depends on many parameters including concentration of sulfate ions, ambient temperature, cement type and composition, water cement ratio, porosity and permeability of concrete, and the presence of supplementary cementitious materials. The exposure of concrete structures to the aggressive environments such as sulfate solution can lead to detrimental chemical, microstructural, and physical changes in the concrete matrix, resulting in serious deterioration [3]. It is generally accepted that exposure of concrete to a sulfate environment elicits two principal reactions: the reaction of sulfate ions and portlandite to form gypsum [18] and that of theresultant gypsum with calcium aluminate hydrates to form ettringite [11]. The effects of sulfate attack on the blended cement incorporating supplementary cementitious materials, such as fly ash, slag, metakaolin, and silica fume have been investigated [2, 7, 12, 13]. According to the available current literature, several researchers have confirmed that the incorporation of supplementary cementitious materials as partial replacement of OPC is a beneficial technique to improve the resistance of concrete to sulfate attack. For this reason, it is important to study the effect of RHA blended cement under sodium sulfate attack. In this investigation, thermal analysis and x-ray diffraction was used to evaluated the concrete containing 10% RHA replacement under sodium sulfate through wetting and drying cycles.

2 Materials and Methods

2.1 OPC

The ordinary Portland cement (OPC) used in this investigation satisfying the requirements of BS EN 197–1 [6] specification for ordinary and rapid-hardening Portland cement. The OPC was supplied in one batch for the entire study and kept in airtight containers to ensure consistent quality and properties. The chemical composition of the OPC used in this study was within the standard range of 70% CaO, 17.8% SiO_2, 3.9% Al_2O_3, 3.2% Fe_2O_3, 1.5% MgO, and 3.6% SO_3. The OPC also indicated a compound composition of 54.5% C_3S, 18.2% C_2S, 9.4% C_3A, and 10.5% C_4AF.

2.2 RHA

The rice husk ash (RHA) used in this study was ground using a laboratory ball mill with porcelain balls. Then, RHA was sieved to obtain ash of 9.52 μm. SiO_2 was identified as the main component of the RHA. In addition, SiO_2, Al_2O_3, and Fe_2O_3 comprised 92% of the material, in accordance with C618-12 [4] of the American Society for Testing and Materials (ASTM), which requires that these three main oxides should comprise no less than 70% of the pozzolanic material.

2.3 Aggregate

A single size (20 mm) of crushed granite was used as the coarse aggregate. The coarse and fine aggregates each had a specific gravity of 2.60 and 2.65, respectively. Where the water absorption rates of 0.47 and 0.85%, correspondingly.

2.4 Sample Preparation and Mix Design

A control mix was prepared using OPC. However, RHA replacement levels of 10% by weight of cement were applied through the study. At the laboratory, RHA was thoroughly mixed with OPC in blended cement, and water was added to the mixer. When the mixtures were prepared, the specimen was cured in water maintained at room temperature for a minimum of 28 days. Then, the specimens were subjected to 5% Na_2SO_4 solution with wetting–drying cycles. The sodium sulfate was prepared by mixing the chemical with distilled water at 5% by weight of volume. According to ACI 318–08 [1], 5% of Na_2SO_4 was representing extremely severe

sulfate exposure. At each cycle (wetting–drying), the solution was replaced by a freshly prepared one or based on the change in the pH of the solution.

2.5 Differential Thermal and Thermo Gravimetric Analysis Test

Differential thermal analysis is corresponding to the thermal decomposition of different phases in paste, whereas thermogravimetric analysis (TGA) measures weight loss caused by decomposition. On the specified day of testing, hardened cement paste samples were crushed into powder form with passing a 75 μm sieve. About 15–20 mg of sample was placed in a platinum pan and heated in a nitrogen atmosphere from 25 to 1000 °C at 10 °C/min. in addition, weight loss which occurs in hardened cement paste due to dehydration and decomposition of its components when heated gradually, was recorded at varying temperatures.

2.6 X-ray Diffraction Test

In accordance with BS EN 13925–1 [5], the samples were scanned in steps of 0.034 °C (2θ) with a fixed counting time of 1 s. The X-ray scan ranged from 2θ = 10 –90 °C using copper (KαCu) with a wavelength λ of 1.5406 nm as the X-ray source. EVA software was used to analyse the phase of the samples.

3 Results and Discussion

3.1 TGA/DTA Analysis

Vedalakshmi et al. [17] have reported that gypsum and ettringite existed in crystal form. In this study, the evidence on the formation of gypsum and ettringite was evaluated by TG–DTA. The graphical illustration representing the TG–DTA of specimens subjected to sodium sulfate solution with cyclic drying-wetting is presented in Fig. 1. The curve of the specimen showed four endothermic peaks. The first endothermic peak positioned between 94.99 and 137.95 °C, with a peak at 104.64 °C and a 5.48% loss of weight, resulted from the dehydration of ettringite and gypsum. According to Skaropoulou et al. [16], the dehydration of ettringite and gypsum from sodium sulfate solution takes place at around 80 and 130 °C. Based on the investigations conducted by Santhanam et al. [15], they found that incorporating pozzolanic material in cement pastes subjected to sulfate solution, the endothermic peak in the range of 80–100 °C is due to the dehydration of ettringite.

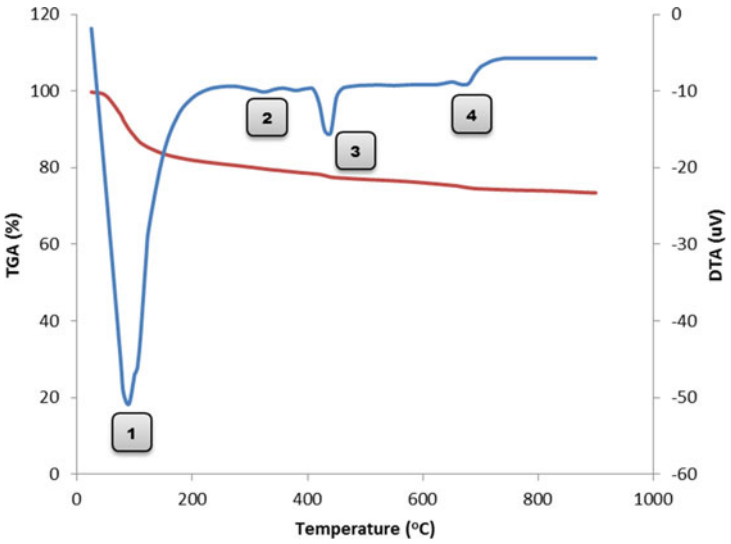

Fig. 1 TGA and DTA curve of RHA blended cement under sodium sulfate subjected to wetting–drying cyclic

The second endothermic peak, located between 277.43 and 357.88 °C, with a peak at 320.69 °C and loss of weight at 1.31%, corresponded to the decomposition of calcium aluminate silicate hydrate, calcium aluminate hydrate, and calcium chloroaluminate. Additionally, the specimen also contained a small peak of brucite, which was confirmed through XRD analysis (see Fig. 2). The endothermic peak at around 358.30 and 401.22 °C, with a peak at 379.16 °C and weight loss of 0.73% was resulted from brucite. The presence of brucite was probably due to the external sulfate attack. The third endothermic peak detected in the range of 410.28–494.15 °C, with a peak at 435.91 °C and weight loss of 1.82%, corresponded to the dehydration of calcium hydroxide. This finding is consistent with the results obtained by Gonçalves et al. [9] who have found that the endothermic peak between 400 and 460 °C is related to the dehydroxylation of the calcium hydroxide. Finally, the endothermic peaks appearing at 641.86 and 713.41 °C, with a peak at 672.78 °C and a 1.67% loss of weight, were associated with the decomposition of calcium carbonate.

3.2 Weight Loss

From the thermogravimetric analysis, the ettringite and gypsum formation were estimated quantitatively. The results are summarized in Table 1, which shows a trend for loss of weight with increasing ettringite and gypsum formation along with

Table 1 Thermo-gravimetric mass losses of cement pastes with different levels of RHA substitution, endothermic peak correspond to ettringite and gypsum

Type of mixes	Age (days)	Temp. range (°C)	Peak temp. (°C)	Weight loss (%)	Onset temp. (°C)	Final temp. (°C)
OPC	3	61.49–100.52	74.65	3.18	64.20	81.78
	7	61.52–119.61	92.50	5.37	78.21	100.28
	28	80.12–122.15	97.54	7.67	88.46	103.25
	56	75.89–130.37	90.49	8.62	84.74	104.06
	90	66.39–113.31	90.49	9.42	87.02	97.95
	180	91.36–137.94	103.61	10.47	96.57	112.24
RHA	3	79.37–126.75	85.74	2.74	79.40	91.07
	7	53.52–111.24	67.74	4.13	54.46	84.82
	28	94.99–137.95	104.64	5.48	87.86	113.58
	56	65.95–91.87	78.33	5.89	67.94	73.00
	90	89.71–130.76	101.50	6.22	95.94	110.76
	180	64.61–94.12	81.27	6.72	70.06	80.44

the increase of exposure period. The results also indicated that the weight losses of RHA blended cement were lower than those found in controlled specimen. This due to the pozzolanic reaction in RHA consumed the $Ca(OH)_2$, which the less amount of $Ca(OH)_2$ decreased the ettringite and gypsum formation. For instance, at early age (i.e. 28 days), the weight loss of the hydrated phases (ettringite and gypsum) was 5.48% (RHA blended cement) and 7.67% (OPC concrete). Based on Table 1, the trend is not consistent for all specimens. This can be explained due to severity of the drying and wetting cycles as used in the current study. Cyclic wetting and drying can increase the rate of corrosion in concrete as a result of two actions. First, cyclic wetting and drying concentrates ions, such as chloride, can increase the rate of corrosion by the evaporation of water during the drying phase [11]. Second, once chloride thresholds have been reached at the depth of cover, drying of the concrete increases the availability of oxygen required for corrosion, because oxygen has a substantially lower diffusion coefficient in saturated concrete [10]. Furthermore, the onset temperature values for the first endothermic peak and the end-set temperature value for the final endothermic peak were also investigated and the results are listed in Table 1.

3.3 XRD Analysis

The sulfate attack on concrete was due mostly to two main reactions: the reaction of Na_2SO_4 and $Ca(OH)_2$ to form gypsum and the reaction of the resulting gypsum with calcium aluminate hydrates to form ettringite. This explanation of the

mechanism of sulfate attack on concrete was confirmed through XRD analysis. The XRD trace indicates that gypsum, ettringite and $Ca(OH)_2$ were only crystalline phases present in the different depths of concrete in addition to quartz and calcium carbonate. Figures 2 and 3 show the XRD results for OPC and RHA blended cement subjected to 5% Na_2SO4 solution with drying-wetting cycles. The peak corresponding to the ettringite ($Ca_6Al_2(SO_4)_3(OH)_{12}\cdot 26H_2O$) was detected at around 16°2θ and 21°2θ. Skaropoulou et al. [16] and Gao et al. [8] found that the peak in the regions from 16.2°2θ to 22.9°2θ was due to ettringite formation. However, a strong intensity peak corresponding to the gypsum ($CaSO_4\cdot 2H_2O$) still appeared at about 18°2θ. Gao et al. [8] reported that the maximum peak at 11.6°2θ and 19.3°2θ indicated the presence of gypsum. The presence of ettringite and gypsum in concrete subjected to sulfate solution showed that these parameters were the main corrosion products. On the other hand, a small amount of thaumasite ($Ca_3Si(OH)_6(CO_3)(SO_4)\cdot 12H_2O$) can be found in the XRD patterns of specimen exposed to Na_2SO_4 solutions. Ettringite and thaumasite have similar crystal structures [18], thus, their XRD patterns show similarities in intensity peaks. In this study, the corresponding peaks of thaumasite were observed at around 16.5°2θ. Finally, the corresponding peaks of calcium carbonate ($CaCO_3$), calcium hydroxide ($Ca(OH)_2$) and quartz (SiO_2) appeared at about 33°2θ, 34°2θ and 47°2θ, respectively. The results also showed that the concentrations of ettringite and gypsum in RHA replacement cement were lower than that in the OPC specimen. This explains the trend exhibited in Figs. 2 and 3. It can be seen that the addition of RHA in blended cement reduced the deterioration of concrete caused by sulfate attack, which could be attributed to the pozzolanic reaction in rice husk ash. When RHA is mixed with cement in concrete, it combines with free lime during the hydration of

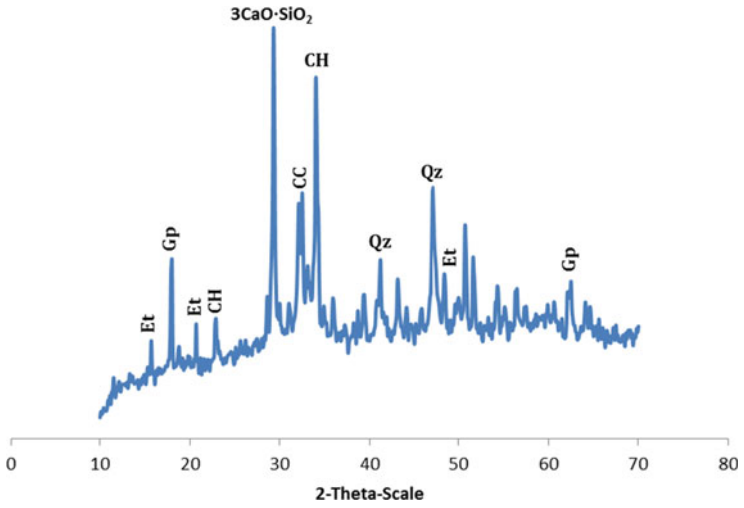

Fig. 2 XRD patterns of the ordinary Portland cement paste subjected to sodium sulfate solution with drying-wetting cycles

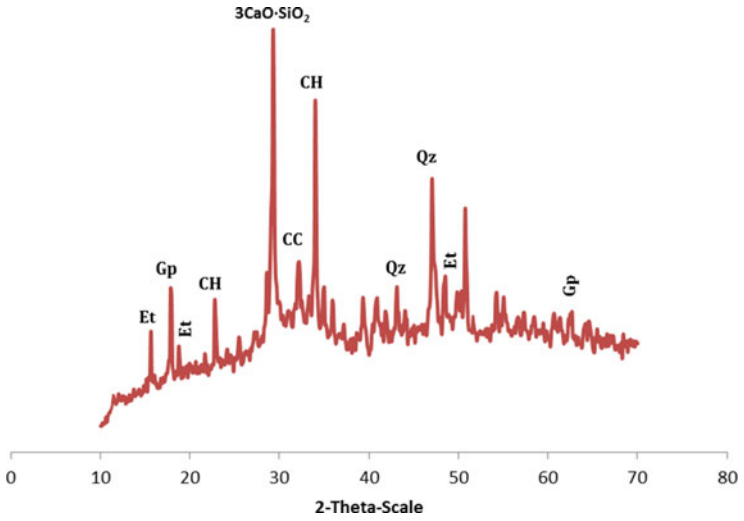

Fig. 3 XRD patterns of RHA blended cement paste subjected to sodium sulfate solution with drying-wetting cycles

cement in concrete to form calcium silicate hydrate (CSH). Similarly, the intensity peak of $Ca(OH)_2$ was found less than that of the OPC concrete due to the pozzolanic reaction. Because of the pozzolanic reaction, the specimen containing RHA had lower $Ca(OH)_2$ content than that of the OPC concrete. This lessened the amount of $Ca(OH)_2$ and subsequently decreased ettringite and gypsum formation. Cement replacement also reduced the overall amount of C_3A in the system and amount of ettringite and gypsum that formed upon sulfate attack.

4 Conclusions

The addition of RHA was found to decrease calcium hydroxide formation by hydration and, consequently, gypsum and ettringite were reduced during sulfate attack. The test results also demonstrated that the amount of calcium hydroxide in RHA blended cement was lower than that of Portland cement. This finding proposed that RHA could be used as an effective mineral addition in the design of durable concrete under sodium sulfate with drying-wetting cyclic condition. In addition, the cyclic exposure to sulfates attack increased the rate of deterioration of ordinary Portland cement which was confirmed by TGA, DTA and XRD analysis.

Acknowledgements The support provided by Malaysian Ministry of Higher Education and Universiti Malaysia Pahang in the form of a research grant (RDU/UMP) vote number RDU190339 for this study is highly appreciated.

References

1. ACI 318-08 (2012) Building Code Requirements for Structural Concrete and Commentary. American Concrete Institute, Farmington Hills, USA
2. Al-Akhras NM (2006) Durability of metakaolin concrete to sulfate attack. Cem Concr Res 36:1727–1734
3. Al-Dulaijan SU, Maslehuddin M, Al-Zahrani MM, Sharif AM, Shameem M, Ibrahim M (2003) Sulfate resistance of plain and blended cements exposed to varying concentrations of sodium sulphate. Cement Concr Compos 25:429–437
4. ASTM C618–08 (2012) Standard Specification for Coal Fly Ash and Raw or Calcined Natural Pozzolan for Use in Concrete. American Society for Testing and Materials, West Conshohocken, PA 19428–2959, United States
5. BS EN 13925–1 (2003) Non-destructive testing. X-ray diffraction from polycrystalline and amorphous materials. General principles, British European Standard, London, United Kingdom
6. BS EN 197–1 (2000) Cement. Composition, Specifications and Conformity Criteria for Common Cements, British European Standard, London, United Kingdom
7. Chatveera B, Lertwattanaruk P (2009) Evaluation of sulfate resistance of cement mortars containing black rice husk ash. J Environ Manage 90:1435–1441
8. Gao X, Ma B, Yang Y, Su A (2008) Sulfate attack of cement-based material with limestone filler exposed to different environments. J Mater Eng Perform 17:543–549
9. Gonçalves JP, Toledo Filho RD, Fairbairn EMR (2008) Evaluation of magnesium sulphate attack in mortarmetakaolin system by thermal analysis. J Therm Anal Calorim 94:511–516
10. Macphee D, Diamond S (2003) Thaumasite in cementitious materials. Cement Concr Compos 25:805–807
11. Marchand J, Samson E, Maltais Y, Beaudoin JJ (2002) Theoretical analysis of the effect of weak sodium sulfate solutions on the durability of concrete. Cement Concr Compos 24:317–329
12. Najimi M, Sobhani J, Pourkhorshidi AR (2011) Durability of copper slag contained concrete exposed to sulfate attack. Constr Build Mater 25:1895–1905
13. Sahmaran M, Erdem TK, Yaman IO (2007) Sulfate resistance of plain and blended cements exposed to wetting–drying and heating–cooling environments. Constr Build Mater 21:1771–1778
14. Santhanam M, Cohen MD, Olek J (2001) Sulphate attack research-whiter now? Cem Concr Res 31:845–851
15. Santhanam M, Cohen MD, Olek J (2003) Mechanism of sulfate attack: a fresh look: Part 2. Proposed Mech Cement Concrete Res 33:341–346
16. Skaropoulou A, Kakali G, Tsivilis S (2006) A study on thaumasite form of sulfate attack (TSA) using XRD, TG and SEM. J Therm Anal Calorim 84:135–139
17. Vedalakshmi R, Sundara Raj A, Palaniswamy N (2008) Identification of various chemical phenomena in concrete using thermal analysis. Indian J Chem Technol 15:388–396
18. Zuquan J, Wei S, Yunsheng Z, Jinyang J, Jianzhong L (2007) Interaction between sulfate and chloride solution attack of concretes with and without fly ash. Cem Concr Res 37:1223–1232